Effect of Ionizing Radiation on the Redox Chemistry of Penta- and Hexavalent Americium

Gregory P. Horne, Travis S. Grimes, William F. Bauer, Christopher J. Dares, Simon M. Pimblott, Stephen P. Mezyk, and Bruce J. Mincher.

UV-Vis Spectra

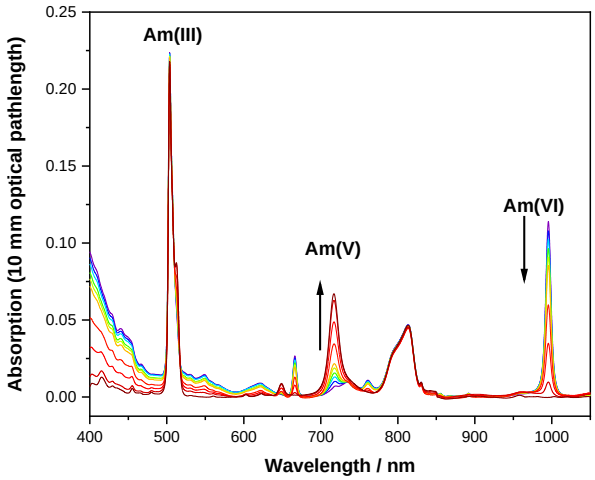

Figure S1. Complimentary UV-Vis absorption spectra for manuscript **Figure 2** - gamma radiolysis (1.19 Gy s^{-1}) of 2 mM americium in aerated 3.0 M HNO_3. Arrows indicate the change in absorption peak growth or decay.

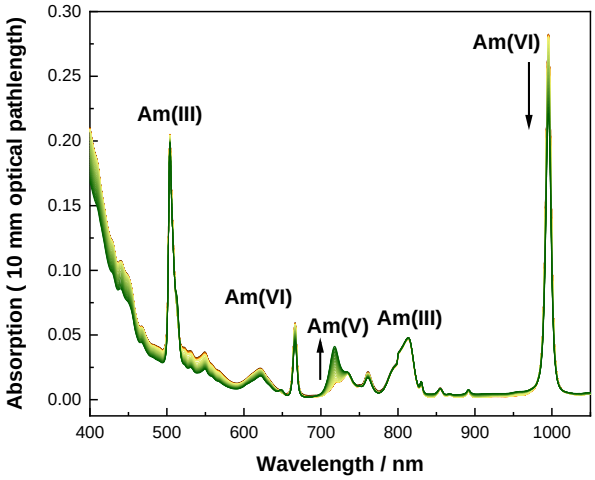

Figure S2. Complimentary UV-Vis absorption spectra for manuscript **Figure 3** – alpha self-radiolysis (7.47×10^{-3} Gy s^{-1}) of 4 mM americium in aerated 3.0 M HNO_3. Arrows indicate the change in absorption peak growth or decay.

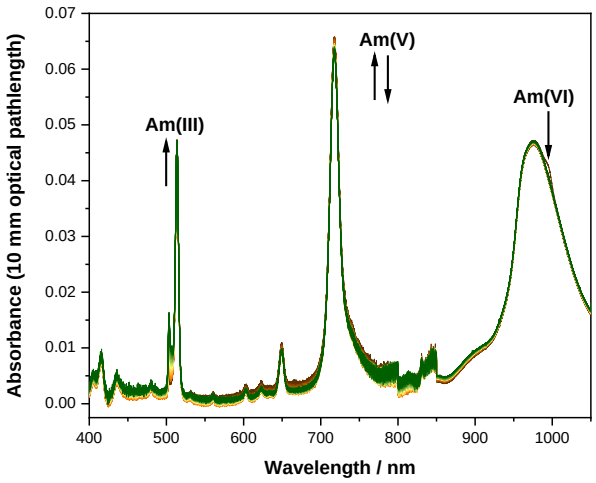

Figure S3. Complimentary UV-Vis absorption spectra for manuscript **Figure 4** – alpha self-radiolysis (2.37×10^{-3} Gy s^{-1}) of 1.39 mM americium in aerated 1.0 M HNO_3. Arrows highlight Am(VI) shoulder peak and its decay, and the change in absorption peak growth or decay of Am(III) and Am(VI).

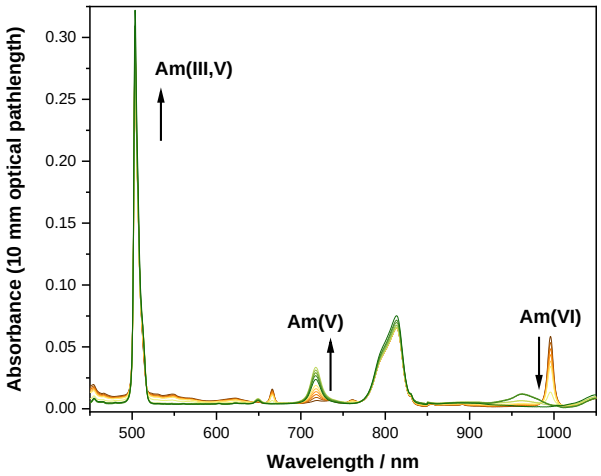

Figure S4. Complimentary UV-Vis absorption spectra for **Figure S9** – gamma radiolysis (1.15 Gy s^{-1}) of 2 mM americium in aerated 1.0 M HNO_3. Arrows indicate the change in absorption peak growth or decay.

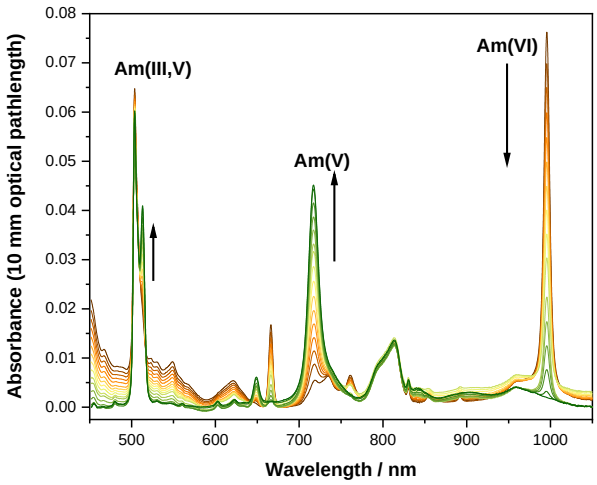

Figure S5. Complimentary UV-Vis absorption spectra for **Figure S10** – gamma radiolysis (1.14 Gy s^{-1}) of 1 mM americium in aerated 3.0 M HNO_3. Arrows indicate the change in absorption peak growth or decay.

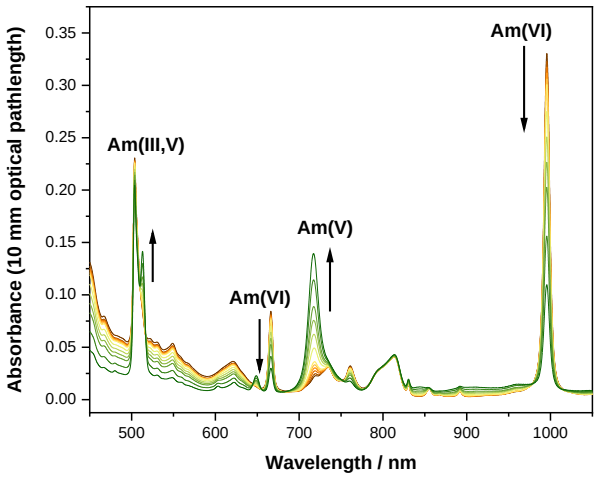

Figure S6. Complimentary UV-Vis absorption spectra for **Figure S11** – gamma radiolysis (1.15 Gy s^{-1}) of 4 mM americium in aerated 3.0 M HNO_3. Arrows indicate the change in absorption peak growth or decay.

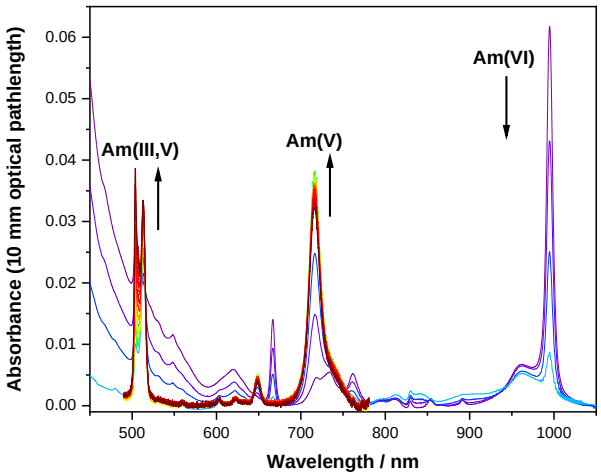

Figure S7. Complimentary UV-Vis absorption spectra for **Figure S12** – gamma radiolysis (0.93 Gy s^{-1}) of 1 mM americium in aerated 6.5 M HNO_3. Arrows indicate the change in absorption peak growth or decay. A higher resolution scan rate was used for the irradiation of Am(V) and subsequent reduction. The initial scans with the larger wavelength window were made only to verify the reduction of Am(VI) induced by gamma irradiation.

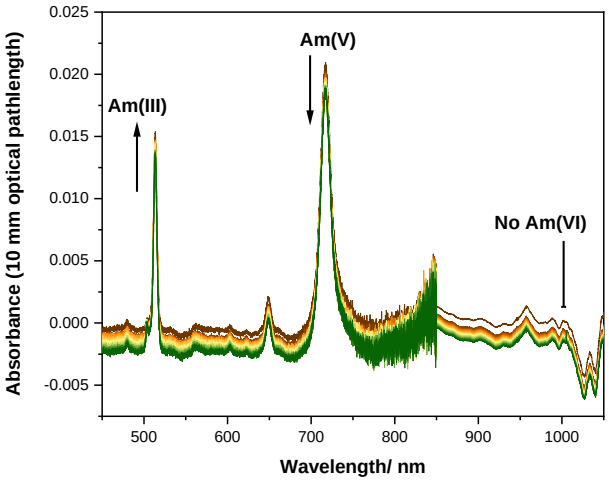

Figure S8. Complimentary UV-Vis absorption spectra for **Figure S13** – alpha self-radiolysis (9.09×10^{-4} Gy s^{-1}) of 0.48 mM americium in aerated 3.0 M HNO_3. Arrows highlight absence of an Am(VI) peak and the change in absorption peak growth and decay of Am(III) and Am(V).

Gamma Irradiations

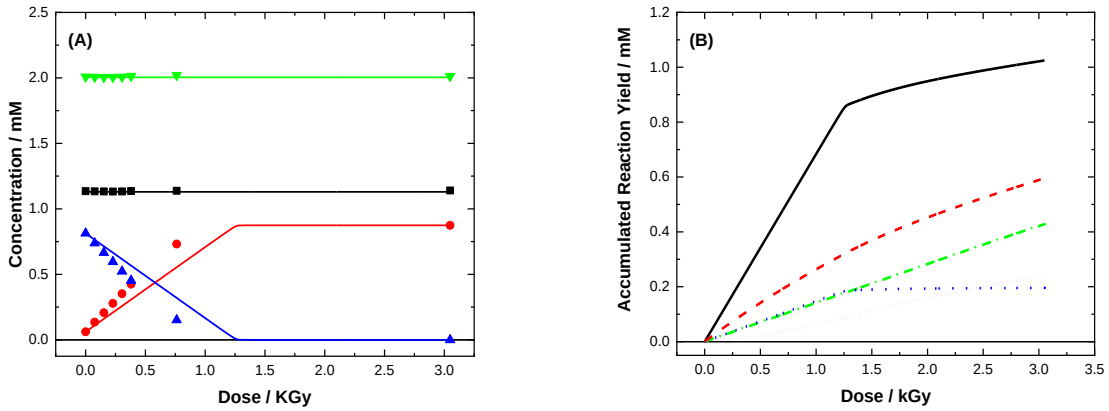

Figure S9. (A) Concentration of Am(III) (■), Am(V) (●), Am(VI) (▲), and Am mass balance (▼) as a function of absorbed dose for the gamma radiolysis (1.19 Gy s^{-1}) of 2 mM americium in aerated 1.0 M HNO_3. Complementary absorption spectra are shown in **Figure S4**. Solid lines are predicted values from multi-scale modelling calculations. **(B)** Calculated accumulated americium reaction kinetics: Am(VI) + HNO_2 (**Solid Black**), Am(VI) + H_2O_2 (**Dashed Red**), Am(VI) + $HO_2^{\bullet}$ (**Dotted Blue**), Am(V) + $^{\bullet}NO_3$ (**Dot-Dash Green**), and Am(V) + $^{\bullet}OH$ (**Short-Dotted Magenta**).

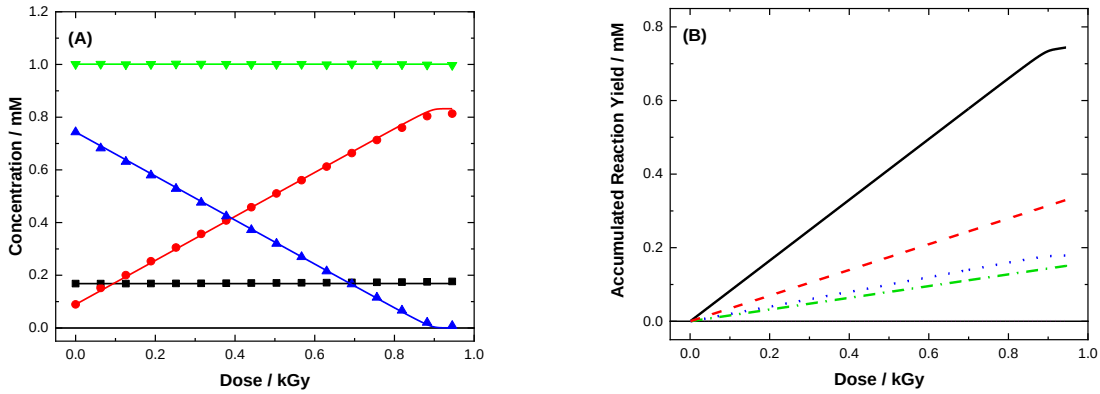

Figure S10. (A) Concentration of Am(III) (■), Am(V) (●), Am(VI) (▲), and Am mass balance (▼) as a function of absorbed dose for the gamma radiolysis (1.14 Gy s^{-1}) of 1 mM americium in aerated 3.0 M HNO_3. Complementary absorption spectra are shown in **Figure S5**. Solid lines are predicted values from multi-scale modelling calculations. **(B)** Calculated accumulated americium reaction kinetics: Am(VI) + HNO_2 (**Solid Black**), Am(VI) + H_2O_2 (**Dashed Red**), Am(VI) + $HO_2^{\bullet}$ (**Dotted Blue**), Am(V) + $^{\bullet}NO_3$ (**Dot-Dash Green**), and Am(V) + $^{\bullet}OH$ (**Short-Dotted Magenta**).

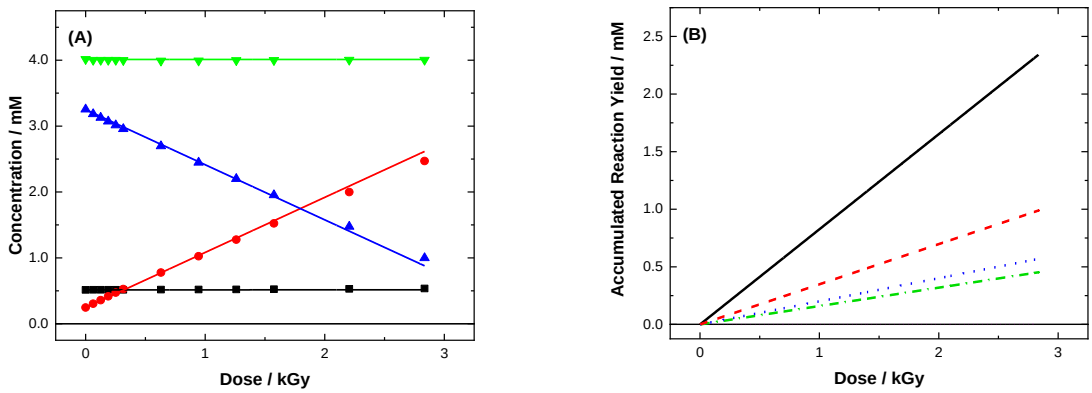

Figure S11. (A) Concentration of Am(III) (■), Am(V) (●), Am(VI) (▲) and Am mass balance (▼) as a function of absorbed dose for the gamma radiolysis (1.15 Gy s^{-1}) of 4 mM americium in aerated 3.0 M HNO_3. Complementary absorption spectra are shown in **Figure S6**. Solid curves are predicted values from multi-scale modelling calculations. **(B)** Calculated accumulated americium reaction kinetics: Am(VI) + HNO_2 (**Solid Black**), Am(VI) + H_2O_2 (**Dashed Red**), Am(VI) + $HO_2^{\bullet}$ (**Dotted Blue**), Am(V) + $^{\bullet}NO_3$ (**Dot-Dash Green**), and Am(V) + $^{\bullet}OH$ (**Short-Dotted Magenta**).

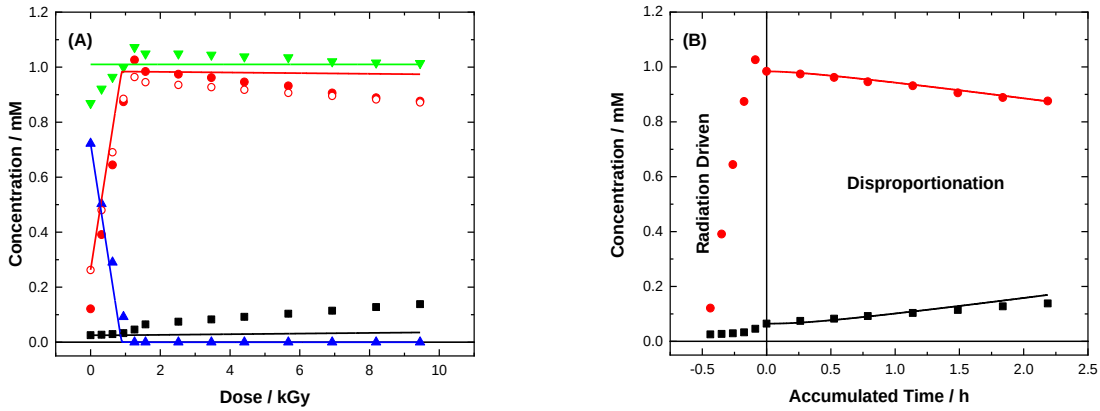

Figure S12. (A) Concentration of Am(III) (■), Am(V) (●), corrected Am(V) (○), Am(VI) (▲), and Am mass balance (▼) as a function of absorbed dose for the gamma radiolysis (0.93 Gy s^{-1}) of 1 mM americium in aerated 6.5 M HNO_3. Complementary absorption spectra are shown in **Figure S7**. **(B)** Concentration of Am(III) (■) and Am(V) (●) as a function of time to highlight the transition from radiolytically driven processes to disproportionation. Solid lines in both figures are predicted values from multi-scale modelling calculations.

Alpha Self-Radiolysis Irradiations

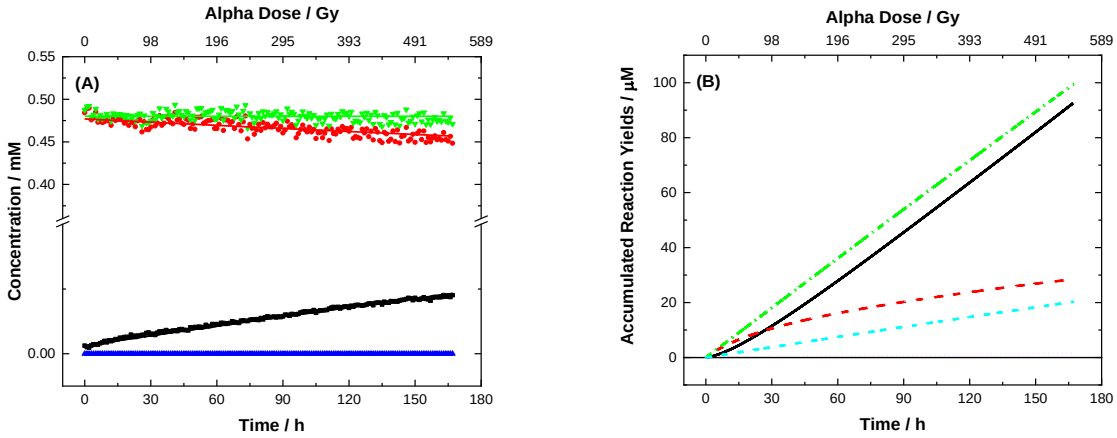

Figure S13. (A) Concentration of Am(III) (■), Am(V) (●), Am(VI) (▲), and Am mass balance (▼) as a function of time for the alpha self-radiolysis (9.09×10^{-4} Gy s^{-1}) of 0.48 mM americium in aerated 3.0 M HNO_3. Complementary absorption spectra are shown in **Figure S8**. Solid lines are predicted values from multi-scale modelling calculations. **(B)** Calculated accumulated americium reaction kinetics: Am(VI) + HNO_2 (**Black Solid**), Am(VI) + H_2O_2 (**Dashed Red**), Am(V) + $^{\bullet}NO_3$ (**Dot-Dash Green**), Am(V) + $^{\bullet}OH$ (**Short-Dotted Magenta**), and Am(V) disproportionation (**Short-Dash-Dot Cyan**).